2010 IEEE International Conference on Robotics and Automation
Anchorage Convention District
May 3-8, 2010, Anchorage, Alaska, USA

A Probability Density Function Approach to Distributed Sensors' Path Planning

S. Ferrari, G. Foderaro, and A. Tremblay

***Abstract*— A novel artificial-potential function approach is presented for planning the paths of distributed sensor networks in a complex dynamic environment. The approach implements a novel potential function generated from a probability density function (PDF) parameterized by an adaptive Gaussian mixture that is optimized to meet network-level objectives, such as cooperative track detection. The PDF represents the goal density that would be obtained by sampling a statistically-significant number of sensors from the mixture. However, since a smaller number of sensors may be deployed, and each sensor is represented by a disk, the potential function is generated by multiplying the PDF by a likelihood update model that produces networks with disjoint fields-of-view. The approach is demonstrated through numerical simulations involving ocean sensor networks deployed in a region of interest near the New Jersey coast.**

I. Introduction

The problem of cooperative track detection, originally introduced in [1], is concerned with the probability that a target track is detected by means of multiple independent sensor detections, at various moments in time. It is motivated by surveillance systems in which little or no prior information is available about the targets, and the sensor obtain elementary target detections that are both infrequent and prone to false alarms [1]–[4]. Therefore, a track is declared detected when it is estimated by fusing multiple independent detections according to an assumed spatio-temporal model. By this approach, the tracks of targets unknown in number can be formed from data of multiple consecutive frames of observations that are collected by simple, low-cost (e.g. passive) sensors, using multiple hypothesis tracking (MHT) [5] or geometric invariants [3] algorithms.

The probability of cooperative track detection in a polygonal region of interest, also known as track coverage [2], is the probability of obtaining multiple independent detections from one or more targets that are assumed to traverse the region with constant speed and heading. It was shown in [4] that, when the number of sensors is very large, the probability of cooperative track detection is given by an integral function of the sensors' density, represented by a joint probability density function (PDF) of the sensors' positions in the region of interest. Recently, several authors addressed the fundamental problem of finding the sensors' ranges and positions that maximize the probability of track detection [1], [2], [6]. When the sensors are static, an approximately optimal sensors' distribution can be determined in the form of a parameterized Gaussian mixture by computing the mixing proportions via sequential quadratic programming [6]. As shown in Section III, when the sensors are dynamic, the probability of track detection can be integrated over time, and optimized with respect to a time-varying Gaussian mixture using a finite number of collocation points. In this case, however, the resulting PDF cannot be sampled to obtain individual sensor positions, because the optimal positions change over time.

Therefore, this paper presents an artificial-potential approach that utilizes the time-varying PDF, provided in the form of a Gaussian mixture, to generate near-optimal sensor trajectories. Another novel potential function is defined from the potential flow of the region of interest, for the purpose of minimizing the power required by the sensors to move in a current velocity field, representing a water body, or the atmosphere.

Potential field is a well-known obstacle-avoidance technique that has been demonstrated very effective for online robot-motion planning in [7]–[9]. In robot-motion planning the objective is to avoid collisions with obstacles that are sensed during the motion, while navigating toward a goal position or configuration [10]. Although the potential field method is well suited to online motion planning and to convergence analysis, its effectiveness is limited by the tendency of the robot to get stuck in local minima of the potential function, e.g., due to narrow passages between closely-spaced obstacles, and oscillations in the presence of obstacles. One of the most effective approaches for escaping these local minima is to "fill" them, and to follow a new local path generated via random-walk algorithms. This paper shows how, after the Gaussian mixture is optimized by the approach presented in [6], the potential field approach can be used to efficiently compute collision-free paths for the individual sensors, such that their probability of detection is maximized, and their power required is minimized.

The paper is organized as follows. The mathematical models, and the problem formulation are described in Section II. The methodology for computing the time-varying Gaussian-mixture PDF from the probability of cooperative track detection is reviewed in Section III. The novel potential-field methodology for computing sensors' trajectories that follow a time-varying PDF, while minimizing energy, is presented in Section IV. The methodology is demonstrated in Section V by applying the potential-field approach to a mobile sensor network deployed in a region of interest near the New Jersey coast, with ocean currents simulated using real coastal ocean dynamics applications radar (CODAR) data.

S. Ferrari and G. Foderaro are with the Laboratory for Intelligent Systems and Control (LISC), Department of Mechanical Engineering and Materials Science, Duke University, Durham, NC 27708-0005, {sferrari, greg.foderaro, andrew.tremblay}@duke.edu

II. Mathematical Models And Problem Formulation

This paper considers the problem of planning the paths of a cooperative network or *field* of n mobile sensors. The sensors are deployed in a rectangular region of interest (ROI) for the purpose of tracking and detecting passive targets during a time interval $[t_0,\ t_f]$. The sensors' optimal distribution is represented by a time-varying PDF $f_{\mathbf{x}}(\mathbf{x}_j, t)$ that is computed by the distributed search approach presented in [6], and reviewed in Section III. The ROI, denoted by $\mathcal{W} = [0,\ L] \times [0,\ L] \subset \mathbb{R}^2$, is populated by N fixed and convex obstacles $\{\mathcal{B}_1, \ldots, \mathcal{B}_N\} \subset \mathcal{W}$ that are not necessarily known *a priori*, but may be detected at any time $t \in [t_0,\ t_f]$. Therefore, the sensors must avoid obstacles and mutual collisions while following the optimal density $f_{\mathbf{x}}(\mathbf{x}_j, t)$ with minimum power required.

Every sensor consists of an autonomous underwater vehicle (AUV) equipped with an on-board passive sensor that moves according to the dynamical model,

$$M(\mathbf{x}_j)\ddot{\mathbf{x}}_j + h(\mathbf{x}_j, \dot{\mathbf{x}}_j) + g(\mathbf{x}_j) = u(\mathbf{x}_j),\ j = 1, \ldots, m \quad (1)$$

where $M(\mathbf{x}_j)$ is the robotic sensor's inertia matrix, $h(\mathbf{x}_j, \dot{\mathbf{x}}_j)$ is the fictitious force, $g(\mathbf{x}_j)$ is the gravitational force, and $u(\mathbf{x}_j)$ is the torque input [9], [11]. The AUV is subject to the ocean currents and, thus, its velocity in inertial frame is $\dot{\mathbf{x}}_j = \boldsymbol{\nu}_j + \boldsymbol{v}_j$, where $\boldsymbol{\nu}_j \in \mathbb{R}^2$ is the velocity vector in body coordinate frame (fixed to the vehicle), and $\boldsymbol{v}_j \in \mathbb{R}^2$ is the local current velocity vector. As shown in [12], [13], the instantaneous AUV's power required is proportional to $\boldsymbol{\nu}_j \in \mathbb{R}^2$, and can be represented by a quadratic cost,

$$e[\boldsymbol{\nu}_j(t)] = \boldsymbol{\nu}_j^T(t)\mathbf{R}\boldsymbol{\nu}_j(t) \quad (2)$$

that penalizes large power dissipations more heavily than small dissipations [14, pg.190]. Where, $\mathbf{R} \in \mathbb{R}^{2\times 2}$ is a diagonal weighting matrix that, in this paper, is chosen as $\mathbf{R} = w_{\mathcal{E}}\ \mathbf{I}_2$, where $\mathbf{I}_2$ is a 2×2 identity matrix, and $w_{\mathcal{E}}$ is a constant energy weight. Then, the power required by the network of AUVs during the interval $[t_0,\ t_f]$ is given by the integral cost,

$$\begin{aligned}\mathcal{E}[\dot{\mathbf{x}}_j(t), t_0, t_f] &= w_{\mathcal{E}} \int_{t_0}^{t_f} \sum_{j=1}^{m} [\dot{\mathbf{x}}_j(t) - \boldsymbol{v}_j(t)]^T \\ &\times \mathbf{I}_2[\dot{\mathbf{x}}_j(t) - \boldsymbol{v}_j(t)]dt \quad (3)\end{aligned}$$

where, $\boldsymbol{v}_j(t)$ is estimated from the forecast models of the ocean dynamics, and on-line measurements, as explained in Section IV.

The signal received by the jth sensor at $\mathbf{x}_j$ is isotropic energy attenuated by the environment according to the following power law,

$$E_j(t) = cF[\lambda_j(t)]^{-\alpha} \quad (4)$$

where, $\lambda_j(t)$ is the distance between the jth sensor and the target at time t. The attenuation coefficient α and the scaling constant c depend on the physical mechanisms of wave propagation and on the environmental conditions, and are assumed to be known and constant in this paper. F represents the target source level, and is assumed to be independent of both time and sensor location [3], [15]. Then, a closest-point-of-approach (CPA) detection is said to take place when E_j exceeds a threshold ϑ_j, which is typically tuned by an operator [16]. At the CPA detection time, the values of E_j and $\mathbf{x}_j$ are reported by the jth sensor to the central processor. From (4), the maximum range at which the jth sensor can report a CPA detection, given a target source level F and a threshold ϑ_j, is $r_j = (cF)^{1/\alpha}\vartheta_j$. Thus, neglecting the effects of the AUV propulsion on sensing, the value of r_j can be estimated from the environmental conditions, and can be assumed known and constant for all $j = 1, \ldots, n$ [2], [4].

It follows that a CPA detection may be reported by the jth sensor only if the target comes within its maximum range r_j. Therefore, for an omnidirectional sensor that obeys the isotropic law (4), the field-of-view (FOV) at time t is a disk of constant radius r_j, centered at $\mathbf{x}_j$, and denoted by $C_j(t) = C_j[\mathbf{x}_j(t), r_j]$ [4]. As schematized in Fig. 1, the sensor can then be viewed as a disk that moves in $\mathcal{W}$ according to the dynamic equation (1). The FOVs of all sensors in the network are represented by the set $S(t) = \{C_1(t), \ldots, C_n(t)\}$, which is specified by the n ranges $r_1(t),\ \ldots,\ r_n(t)$, and the n state vectors $\mathbf{x}_1(t), \ldots, \mathbf{x}_n(t)$. As a result, the network's probability of cooperatively detecting tracks of unauthorized targets in $\mathcal{W}$ was recently shown in [2], [4] to be a function of the sensors' ranges and positions.

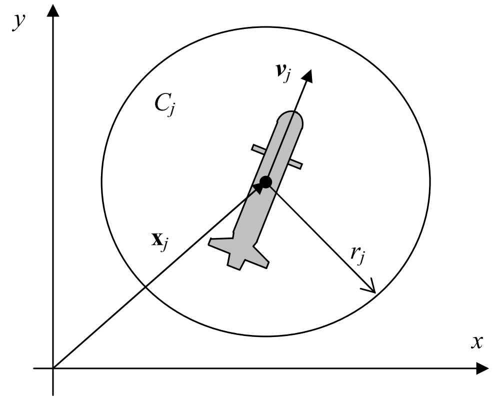

Fig. 1. Schematic of jth mobile sensor (not to scale) taken from [17].

As reviewed in the next section, when n is very large, the network's state and probability of detection can be formulated in terms of the sensors' distribution, which can be conveniently represented by a parameterized Gaussian mixture [6]. This paper shows how, after the Gaussian mixture is optimized by the approach presented in [6], it can be used to efficiently compute collision-free paths for the individual sensors, such that their probability of detection is maximized, and their power required is minimized.

III. Background on Cooperative Track Detection

The problem of cooperative track detection was first introduced in [1], and is concerned with the probability that a target track is detected by a cooperative sensor network by obtaining multiple elementary (e.g. CPA) detections at various moments in time. A track is stated as detected when it can be formed or estimated by fusing multiple detections according to an assumed spatio-temporal model of the target tracks. With this methodology, the tracks of an unknown number of targets can be assembled from multiple consecutive frames of observations. This data can be collected by simple, low-cost (e.g. passive) sensors, using MHT [5] or geometric invariants [3] algorithms.

The dimensions of $\mathcal{W}$ and the time interval ΔT are chosen such that the target can be assumed to move at a constant speed V and heading θ, and to maintain a constant source amplitude. After a minimum of k detections are obtained from k distinct sensors in the network, the values of E_j and $\mathbf{x}_j$ are fused by a central processor to estimate the target track [3]. The number of required target detections k depends on the false-alarm rate, on the measurement errors, and on the track accuracy required by the surveillance system [3]. A value of $k = 3$ was found to provide accurate tracking by proximity sensors subject to few false alarms, and errors normally distributed with a standard deviation of 20% [3].

When n is very large, the probability of cooperative track detection, also known as track coverage [2], can be derived by the distributed search approach presented in [4]. This approach assumes that all n sensors have the same range, $r_j = r$ for all j, and that the probability of detection of the jth sensor is equal to one everywhere inside $\mathcal{C}_j(t)$ at t, and is equal to zero elsewhere. The sensors' state and the targets' speeds, headings, and initial positions are considered as random variables described by the joint PDFs $f_{\mathbf{x}}(\mathbf{x}_j, t)$, $f_V(V, t)$, $f_\theta(\theta, t)$, and $f_T(\mathbf{x}_{T_0}, t)$, respectively. The PDF of the sensors' state is a function of time, because the sensors move to optimize their probability of track detection. The PDFs of the target track's parameters are assumed to be known functions of time that are obtained from the aforementioned target-tracking algorithms [3], [5]. Then, the detection region $\Omega_T \subset \mathcal{W}$ can be grown isotropically from the target track,

$$\mathbf{x}_T(t) = \mathbf{x}_{T_0} + V[\cos\theta \ \ \sin\theta]^T dt \tag{5}$$

over a time differential $dt \subset [t_0, \ t_f]$, where $\mathbf{x}_T(t_0) = \mathbf{x}_{T_0} \in \mathcal{W}$. Let the event $D_j = \{1, \ 0\}$ represent the set of all possible mutually-exclusive outcomes corresponding to sensor j reporting (1) or not reporting (0) a target detection. Then, assuming the targets are distributed uniformly in $\mathcal{W}$, the probability of a detection being reported by sensor j is given by a spatial Poisson process,

$$\Pr\{D_j = 1 \mid \mathbf{x}_T(t) \in \mathcal{W}\} = 1 - e^{-\phi_t} \tag{6}$$

where,

$$\phi_t(\mathbf{x}_{T_0}, V, \theta) = \int_{t_0}^{t_f} \int_{\Omega_T(\mathbf{x}_{T_0}, \theta, V dt)} f_{\mathbf{x}}(\mathbf{x}_j, t) d\mathbf{x} dt \tag{7}$$

is the coverage factor for a sensor sampled from $f_{\mathbf{x}}(\mathbf{x}_j, t)$, and with a detection region Ω_T. The coverage factor of a spatial Poisson process is defined as the expected value of the number of points that fall in a small region or subset of a Euclidian space. Where, every point that falls into this region corresponds to a detection event $D_j = 1$.

In a network of n sensors, the set of events $\{D_1, \ldots, D_n\}$ is reported to the central processor to attempt to form a target track, and a successful track detection is declared when $\sum_{j=1}^{n} D_j \geq k$. Thus, the probability of a successful track detection by at least k sensors can be described using Bernoulli trials [4]. Assuming that individual detection events are statistically identical and independent, and that $\phi_t << 1$ and $n >> 1$, the probability of successful track detection in $\mathcal{W}$ can be approximated by an integral function of the sensors' PDF,

$$\begin{aligned} P_t &\equiv \Pr(\sum_{j=1}^{n} D_j \geq k \mid \mathbf{x}_T(t) \in \mathcal{W}) \qquad (8) \\ &\approx 1 - \int_{t_0}^{t_f} \int_{0}^{2\pi} \int_{V_{min}}^{V_{max}} \int_{\mathcal{W}} e^{-n\phi_t(\mathbf{x}_{T_0}, V, \theta)} f_T(\mathbf{x}_{T_0}, t) \\ &\times \ f_V(V, t) f_\theta(\theta, t) \sum_{m=0}^{k-1} \frac{[n\phi_t(\mathbf{x}_{T_0}, V, \theta)]^m}{m!} d\mathbf{x}_{T_0} dV d\theta dt \end{aligned}$$

as shown in [4]. Where, V_{min} and V_{max} are the target's minimum and maximum speeds, respectively, and $\phi_t(\mathbf{x}_{T_0}, V, \theta)$ is a function of $f_{\mathbf{x}}(\mathbf{x}_j, t)$, as shown in (7).

From (8), an approximately optimal sensors' distribution can be determined in the form of a parameterized Gaussian mixture, as shown in [6]. Assume the optimal sensors' distribution be represented by a time-varying finite mixture model of the form

$$\begin{aligned} f_{\mathbf{x}}(\mathbf{x}_j, t) &= \sum_{i=1}^{m} w_i(t) f_i(\mathbf{x}_j, t), \quad 0 \leq w_i(t) \leq 1, \quad \forall i, t \\ & \sum_{i=1}^{m} w_i(t) = 1. \qquad (9) \end{aligned}$$

The weights $w_1(t), \ldots, w_m(t)$ are called the mixing proportions, and $f_1(\mathbf{x}_j, t), \ldots, f_m(\mathbf{x}_j, t)$ are the component densities of the mixture. The component densities are defined such that $f_i(\mathbf{x}_j, t) = 0$ for all i and $\mathbf{x} \notin \mathcal{W}$, and (9) must obey the normalization condition $\int_{\mathcal{W}} f_{\mathbf{x}}(\mathbf{x}_j, t) d\mathbf{x} = 1$ at any t. Then, the probability of track detection P_t can be optimized with respect to the mixing proportions by evaluating (7)-(9) at M equally-spaced collocation points $t_k = t_0 + k\Delta t$, $k = 1, \ldots, M$, where $\Delta t = (t_f - t_0)/M$ is the discretization interval. At every point t_k, the triple integral in (8) is evaluated numerically using a multi-dimensional fast Fourier transform (FFT) algorithm, as shown in [6]. When, the mixture in (9) is discretized with respect to time, it can be represented by mM-mixing proportions represented by the vector of weights $\boldsymbol{\chi} = [w_{11} \ \ldots \ w_{mM}]^T$, where $w_{ik} \equiv w_i(t_k)$.

The numerical optimization of (8) is then reduced to the nonlinear program (NLP),

$$\max_{\boldsymbol{\chi}} \quad P_t(\boldsymbol{\chi}), \tag{10}$$

$$\text{subj. to} \quad \sum_{i=1}^{m} w_{ik} = 1, \ \forall k = 1, \ldots, M \tag{11}$$

$$w_{ik} \geq 0, \ w_{ik} \leq 1, \ \forall k = 1, \ldots, M \tag{12}$$

for which effective sequential quadratic programming (SQP) algorithms are available [18]. The solution of (10)-(12), denoted by $\boldsymbol{\chi}^*$, is an approximately-optimal vector of mixing proportions for the Gaussian mixture (9). By substituting $\boldsymbol{\chi}^*$ in (9), an approximately-optimal PDF $f^*_{\mathbf{x}}(\mathbf{x}_j, t_k)$ is obtained for all t_k, that maximizes the probability of track detection (8) during $[t_0, \ t_f]$. An example of this time-varying finite-mixture PDF with $m = 10$ components, $[t_0, \ t_f] = [0, \ 12]$ hr, is plotted in Fig. 2, at times $t = 0$, 2, and 9 hr.

A methodology based on probabilistic sampling was developed and demonstrated in [6] for placing n static sensors in $\mathcal{W}$, based on an approximately optimal static Gaussian mixture. Although an approximately optimal time-varying Gaussian mixture can be determined from (10), a methodology is not yet available for translating it into sensor paths for dynamical sensors that obey the model in (1). This paper presents a novel path-planning approach inspired by potential field techniques that is described in next section, and can be applied to a network of cooperative mobile sensors as demonstrated by the numerical simulations in Section V.

IV. Probability Density Function Approach To Path Planning

Potential field is well-known approach to robot motion planning that treats the robot as a particle under the influence of an artificial potential field or function, U, that captures the geometric characteristics of an obstacle-populated workspace, or ROI, $\mathcal{W}$. So far, several potential field methods have been developed for generating a collision-free path for a single mobile robot (1) that must travel from an initial configuration to a goal configuration, without a prior model of the obstacles. One advantage of potential field over other motion planning approaches is that it can easily account for obstacles that are sensed *online*, i.e., during the motion execution [10]. Another advantage demonstrated in this paper is that the artificial potential function can be defined based on other geometric objectives that are not necessarily related to obstacles. The main disadvantage of potential field is that the robot follows the direction of steepest descent of U and, therefore, can potentially get stuck at a local minimum. In this case, the method is combined with a graph searching technique, or a random-walk algorithm, to help the robot escape local minima [10].

In existing potential-field techniques, the potential function is the sum of an attractive potential U_{att} that "pulls" the robot toward a goal state $\mathbf{x}_f$, and a repulsive potential U_{rep} that "pushes" robot away from the obstacles [9]. After U is defined, the method is implemented by discretizing the robot workspace $\mathcal{W}$, and by evaluating the potential function for all discrete value of $\mathbf{x}$ in $\mathcal{W}$, using a finite resolution grid [19]. Subsequently, at any time $t_k \in [t_0, \ t_f]$, an artificial force $\mathbf{F}(\mathbf{q})$ that is proportional to the negative gradient of the artificial potential, $-\nabla U(\mathbf{x}_j, t_k)$, is applied to the robot, in order to follow the steepest-descent direction of U.

This paper presents a novel potential field approach that plans the paths of n cooperative sensors, such that they follow (or are "pulled" toward) a time-varying PDF, comprised of the Gaussian mixture (9). The approach generates a novel potential function that is defined as a linear combination of (i) an attractive potential, representing the desired distribution (PDF) of the sensors, (ii) a repulsive potential representing collision avoidance between sensors, and (iii) the potential flow, representing the integral of the ocean current velocity field. This novel potential function differs from those previously presented in the literature in that it is based on the joint PDF of the state of multiple robotic sensors, it is time-varying, and avoids collisions between sensors and multiple obstacles while minimizing the power required to navigate in a known current velocity field.

The attractive potential is defined based on the approximately-optimal PDF, $f^*_{\mathbf{x}}(\mathbf{x}_j, t_k)$, computed from the NLP (10). This PDF represents the goal density of sensors and, when integrated over a region $\mathcal{R} \subset \mathcal{W}$, it provides the probability that the jth sensor is located in $\mathcal{R}$ at t_k, i.e., the probability mass $\Pr(\mathbf{x}_j \in \mathcal{R}, t_k) = \int_{\mathcal{R}} f^*_{\mathbf{x}}(\mathbf{x}_j, t_k) d\mathbf{x}$. In order to obtain independent sensor detections, the sensors' FOV must be disjoint. Thus, the effect of sampling a sensor state $\mathbf{x}_j$ from $f^*_{\mathbf{x}}(\mathbf{x}_j, t_k)$ should downgrade the probability mass corresponding to its FOV, such that if the jth sensor takes a state value, the probability that another sensor in the network takes the same state value is decreased. It was recently shown in [6] that, when n static sensors are placed based on a static PDF, for example, random sampling is not very useful because random samples have an asymptotic relationship with the distribution. Thus, unless a very large number of sensors is deployed, a single realization of the sampling procedure may not be representative of the optimal sensor density.

For this reason, the potential function developed in this paper for mobile sensors is generated from a likelihood update model inspired by [6], and by which a goal posterior PDF is updated by setting a likelihood function, denoted by $L(\cdot)$, equal to zero inside the sensors' FOVs. Let the set $X(t_k) = \{\mathbf{x}_1(t_k), \ldots, \mathbf{x}_n(t_k)\}$ denote all sensors' positions at time t_k. Then, the goal posterior PDF defined as,

$$\pi(\mathbf{x}_j, t_k) = f^*_{\mathbf{x}}(\mathbf{x}_j, t_k) \ L[\mathbf{x}_j, t_k \mid X(t_{k-1})] \tag{13}$$

where,

$$L[\mathbf{x}_j, t_k \mid X(t_{k-1})] \equiv \begin{cases} 0 & \forall \mathbf{x} \in C_j[\mathbf{x}_j(t_{k-1}), r_j], \ \forall j \\ 1 & \text{o.w.} \end{cases} \tag{14}$$

is then used to move the sensors in place of the goal PDF $f^*_{\mathbf{x}}(\mathbf{x}_j, t_k)$. Therefore, in a dynamic sensor network where sensors' state is constantly changing in the ROI, the likelihood and posterior functions are updated over time, at every time step t_k. The model likelihood update model

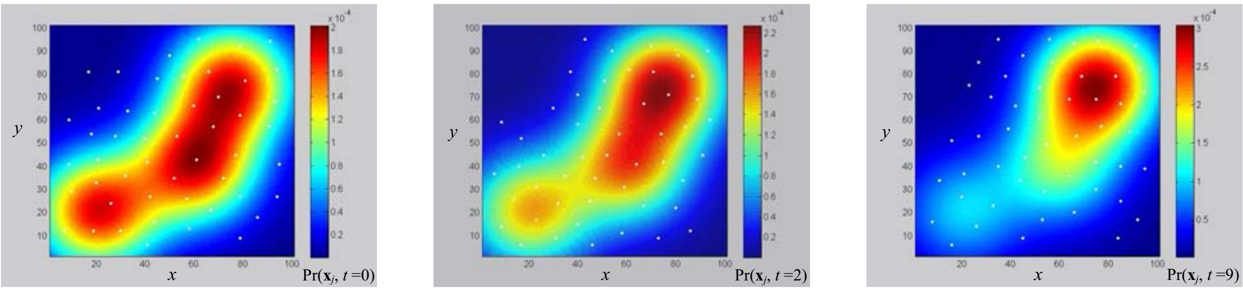

(a)

(b)

(c)

Fig. 2. Example of time-varying finite-mixture PDF with $m = 10$, $[t_0,\ t_f] = [0,\ 12]$ hr, at times $t_k = 0$ hr (a), $t_k = 2$ hr (b), and $t_k = 9$ hr (c).

in (14) effectively “cuts out” circles from the prior PDF based on the sensors’ positions, in order to downgrade the probability that multiple FOVs intersect. Then, the attractive potential is defined as,

$$U_{att}(\mathbf{x}_j, t_k) = -\pi(\mathbf{x}_j, t_k) \tag{15}$$

such that the direction of its steepest descent will lead the sensors to local maxima of the goal PDF $f^*_{\mathbf{x}}(\mathbf{x}_j, t_k)$.

Collisions with a set of fixed obstacles $B(t_k) \equiv \{\mathcal{B}_1, \mathcal{B}_2, \ldots\}$ that are sensed online by the time t_k are avoided by means of an additive repulsive potential that is updated as new obstacles are sensed during $[t_0,\ t_f]$ [20]. Every obstacle $\mathcal{B}_i \in B(t_k)$ in $\mathcal{W}$ maps in the sensor state space $\mathcal{C}$ to a C-obstacle that is defined as the subset of $\mathcal{C}$ that causes collisions with $\mathcal{B}_i$, i.e., $\mathcal{CB}_{ij} \equiv \{\mathbf{x}_j \in \mathcal{C} \mid \mathcal{A}(\mathbf{x}_j) \cap \mathcal{B}_i \neq \emptyset\}$, where $\mathcal{A}(\mathbf{x}_j)$ denotes the subset of $\mathcal{W}$ occupied by the AUV geometry $\mathcal{A}$ when the sensor state is $\mathbf{x}_j$. The union of all C-obstacles in $\mathcal{W}$ is referred to as the C-obstacle region. Thus, the sensors can avoid collisions by remaining in the free configuration space, defined as the complement of the C-obstacle region $\mathcal{CB}$ in $\mathcal{C}$, i.e., $\mathcal{C}_{free} = \mathcal{C} \backslash \mathcal{CB}$ [10]. Then, the repulsive potential for a set of obstacles $B(t_k)$ is defined as,

$$U_{obs}(\mathbf{x}_j, t_k) = \begin{cases} \frac{1}{2}\eta(\frac{1}{\rho(\mathbf{x}_j)} - \frac{1}{\rho_0})^2 & \text{if} \quad \rho(\mathbf{x}_j) \leq \rho_0 \\ 0 & \text{if} \quad \rho(\mathbf{x}_j) > \rho_0 \end{cases} \tag{16}$$

where, $\rho(\mathbf{x}_j)$ is the minimum distance from $\mathbf{x}_j$ to $\mathcal{CB}$ at t_k:

$$\rho(\mathbf{x}_j) = \min_{\mathbf{x} \in \mathcal{CB}_j} \|\mathbf{x}_j - \mathbf{x}\|, \quad \mathcal{CB}_j \equiv \cup_{i=1}^{N} \mathcal{CB}_{ij} \tag{17}$$

$\eta > 0$ is a scaling factor, and $\rho_0 > 0$ is a distance-of-influence parameter that is chosen by the user.

Although the likelihood function (14) already minimizes the probability that multiple sensors take the same state value, for added safety, collisions between the n UAVs are avoided by introducing the repulsive potential,

$$U_{\ell_{rep}}(\mathbf{x}_j, t_k) = \begin{cases} \frac{1}{2}\eta \left(\frac{1}{\rho_{\ell j}(\mathbf{x}_j, t_k)} - \frac{1}{\rho_0}\right)^2 & \text{if} \quad \rho_{\ell j}(\mathbf{x}_j, t_k) \leq \rho_0 \\ 0 & \text{if} \quad \rho_{\ell j}(\mathbf{x}_j, t_k) > \rho_0 \end{cases} \tag{18}$$

where $\rho_{\ell j}$ is the Euclidian distance between the $j$the AUV and the nearest ℓth AUV in the network at time t_k, defined as

$$\rho_{\ell j}(\mathbf{x}_j, t_k) = \min_{\mathbf{x}_\ell} \|\mathbf{x}_j(t_k) - \mathbf{x}_\ell(t_k)\|, \quad \ell = 1, \ldots, n, \quad \ell \neq j. \tag{19}$$

and the other quantities are defined as in Section III.

Finally a potential field defined in terms of the potential flow is introduced in order to minimize the power required in (3), which is proportional to the AUV’s velocity vector in body coordinate frame (i.e. relative to the ocean current). As shown in [12], [13], [21], the ocean currents can be modeled using environmental forecasts with assimilated data [22] in order to exploit the natural dynamics for AUVs’ transport and minimize the power required. Using the approach presented in [21], a smooth functional representation of the current velocity field in $\mathcal{W}$, during the time interval $[t_0,\ t_f]$, can be obtained by training a feedforward neural network (NN),

$$\boldsymbol{v}_j(\mathbf{x}_j, t_k) = \mathbf{W}_2 \boldsymbol{\Phi}(\mathbf{W}_1\ [\mathbf{x}_j^T\ t_k]^T + \mathbf{b}_1) + \mathbf{b}_2 \tag{20}$$

with a given ocean forecast containing estimates of $\boldsymbol{v}_j$ at sample points in space and time. Where the operator $\boldsymbol{\Phi}(\mathbf{n}) \equiv [\sigma(n_1) \ \cdots \ \sigma(n_s)]^T$ represents one hidden layer of s sigmoidal functions, $\sigma(n_i) \equiv 1/(1 + e^{-n_i})$. And, the NN weights $\mathbf{W}_1 \in \mathbb{R}^{s \times 3}$, $\mathbf{W}_2 \in \mathbb{R}^{2 \times s}$, $\mathbf{b}_1 \in \mathbb{R}^s$, and $\mathbf{b}_2 \in \mathbb{R}^2$, are determined by a Bayesian regularization backpropagation algorithm (‘trainbr’ [23]) as demonstrated in [21].

As can be expected, minimum-energy AUVs’ trajectories utilize knowledge of the ocean’s velocity field, thereby minimizing deviations from the trajectories of Lagrangian fluid particles in an irrotational flow with a vector field given by the model (20). The ocean flow velocity $\boldsymbol{v}_j$ is a vector field that is equal to the negative gradient of the velocity potential φ, i.e., $\boldsymbol{v}_j = -\nabla\varphi$ [24]. It follows that the power required by the jth target can be minimized by including an attractive potential given by the potential flow corresponding to the model of ocean currents in (20). Thus, the artificial potential function for sensor j is defined as,

$$\begin{aligned} U(\mathbf{x}_j, t_k) \quad &= \quad w_f\ U_{att}(\mathbf{x}_j, t_k) + U_{obs}(\mathbf{x}_j, t_k) \\ &+ \sum_{\ell=1, \ell \neq j}^{m} U_{\ell_{rep}}(\mathbf{x}_j, t_k) + w_{\mathcal{E}}\ \varphi[\mathbf{x}_j(t_k), t_k], \end{aligned} \tag{21}$$

for all $t_k \in [t_0, t_f]$, where $w_f, w_{\mathcal{E}} > 0$ are constant weights chosen by the user based on the desired tradeoff between the goal of following the PDF $f^*_{\mathbf{x}}(\mathbf{x}_j, t_k)$ and the goal of minimizing the power required. Although the velocity potential could be obtained by integrating (20), in the implementation it is not computed because the paths of the AUVs are computed from the gradient of (21).

According to the potential field approach, the force applied to the jth sensor is proportional to the negative gradient of U at t_k,

$$\mathbf{F}(\mathbf{x}_j, t_k) = -\nabla U(\mathbf{x}_j, t_k) = -\left[\frac{\partial U(\mathbf{x}_j, t_k)}{\partial x_j} \dots \frac{\partial U(\mathbf{x}_j, t_k)}{\partial y_j}\right]^T \quad (22)$$

where $\mathbf{x}_j = [x_j \quad y_j]^T$. However, In this paper, every sensor j is assumed to move with a constant speed relative to a fixed point. This is achieved by using the constant speed value as a reference for a PID controller that returns the appropriate propeller rotational speed to compensate for a changing ocean flow velocity, v_j. Since the speed of sensor j in the workspace is independent of $\mathbf{F}(\mathbf{x}_j, t_k)$, the gradient of the artificial potential U is only used to determine the optimal heading angle of the UUV during $[t_0,\ t_f]$. Sensor j adjusts to the heading angle by using it as a reference for a second PID controller that computes a rudder position. In future work, the method will be further improved such that the artificial potential in (21) may be used directly to compute the control input for the AUV platform. For example, the following time-varying feedback control law,

$$u = -\nabla U(\mathbf{x}_j, t_k) + d(\mathbf{x}_j, \dot{\mathbf{x}}_j) \quad (23)$$

where $d(\cdot)$ is an arbitrary dissipative force, may be adapted from [9], and applied to the jth AUV with dynamic equation (1) for inner-loop control.

V. Simulations And Results

The methodology presented in the previous section is demonstrated here on a simulated ocean sensor network comprised of $n = 12$ sensors and $m = 5$ fixed obstacles deployed at arbitrary positions in a ROI, $\mathcal{W} = [0,\ L_1] \times [0,\ L_2]$ where $L_1 = 90km$ and $L_2 = 82.51\ km$. The simulation was run over the time interval $t \in [t_0, t_f]$ in increments of $t_s = 1\ sec$ with $t_0 = 0$ and $t_f = 9\ hr$. The sensor ranges for all vehicles are set as $r = 5\ km$. The repulsive potential constant η was set as 200, and ρ_0 was chosen as 10 km for the effective distance from other sensors to prevent sensor overlapping and collisions and 5 km for the distance from static obstacles and the ROI boundaries. The mixing proportions were all set to be identical values of 0.0833 with $m = 12$. The time-varying ocean current velocity field within $\mathcal{W}$ was generated from the feedfoward neural network (20) and CODAR data given by COOL at Rutgers University [25]. A snapshot of the velocity field and of the ROI boundaries is shown in Fig. 3.

The goal heading angles of the sensors are set equal to the optimal directions of movement calculated with the method described in Section IV. The gradient of the potential U is estimated by evaluating the potentials at several points around $\mathbf{x}_j$, but the 'gradient' function in MATLAB can also be used. The desired speeds were set to be constant at 2.0 m/s relative to a fixed point, but the vehicle speeds relative to the ocean current velocities, and therefore the propeller rotational speeds, were continuously changed depending on the ocean movements at the AUVs' positions. Figure 5 shows the the positions of the sensors (triangles) at various times during the interval $[t_0,\ t_f]$ illustrating that, by following the negative gradient of the potential, the sensors' density reflects the goal PDF plotted on the background, while avoiding collisions with the obstacles (white squares), and while avoiding mutual collisions or intersections between FOVs (circles). In this simulation, the sensors are initially deployed at arbitrary locations (Fig. 5.a), and subsequently reconfigure based on the PDF by means of the potential field method presented in Section IV. Another possibility is to first place the sensors at a set of n initial positions sampled from $f_{\mathbf{x}_j}(\mathbf{x}_j, 0)$, and then to apply the potential field method in Section IV such that the desired density is followed at all times. The former approach is used here to illustrate the effectiveness of the potential field method. This effectiveness is also demonstrated by plotting the trajectories of the sensors using the artificial potential function in (21) with $w_f = 0$. As shown in Fig. 6, in this case the sensors avoid obstacles and mutual collisions, but never follow the goal PDF, illustrated in Fig. 5.

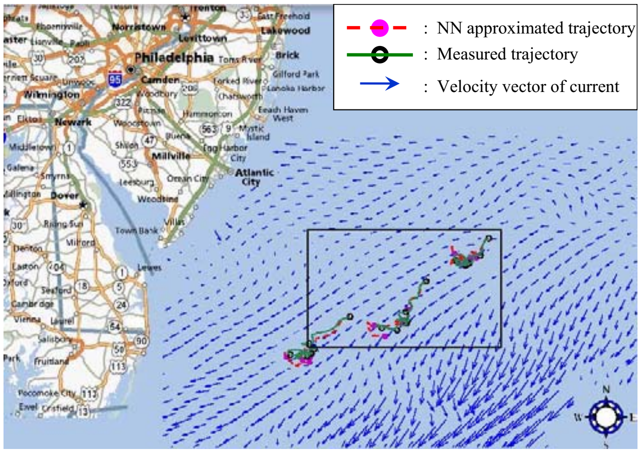

Fig. 3. Example ocean current velocity field obtained from the neural network model and from CODAR measurements in the ROI $\mathcal{W}$ (black rectangle) with longitude of 72.7° W to 74.1° W, and latitude of 38.6° N to 39.5° N (taken from [21]).

Depending on the user's preferences, the behavior of the sensors may be tuned to meet desired criteria. Since the weighting constants, w_f and $w_{\mathcal{E}}$, are included in the artificial potential function, the vehicles can be instructed to favor following the gradients of the PDF over the paths that minimize required energy and vice versa. The effect of changing the weights is demonstrated in Figure 7. When w_f is kept constant and $w_{\mathcal{E}}$ is increased, it is seen that the power consumption decreases significantly. If w_f is set very low relative to $w_{\mathcal{E}}$, as in Fig. 6 where $w_f = 0$, the sensors ignore the PDF and simply follow the ocean currents to minimize the power required.

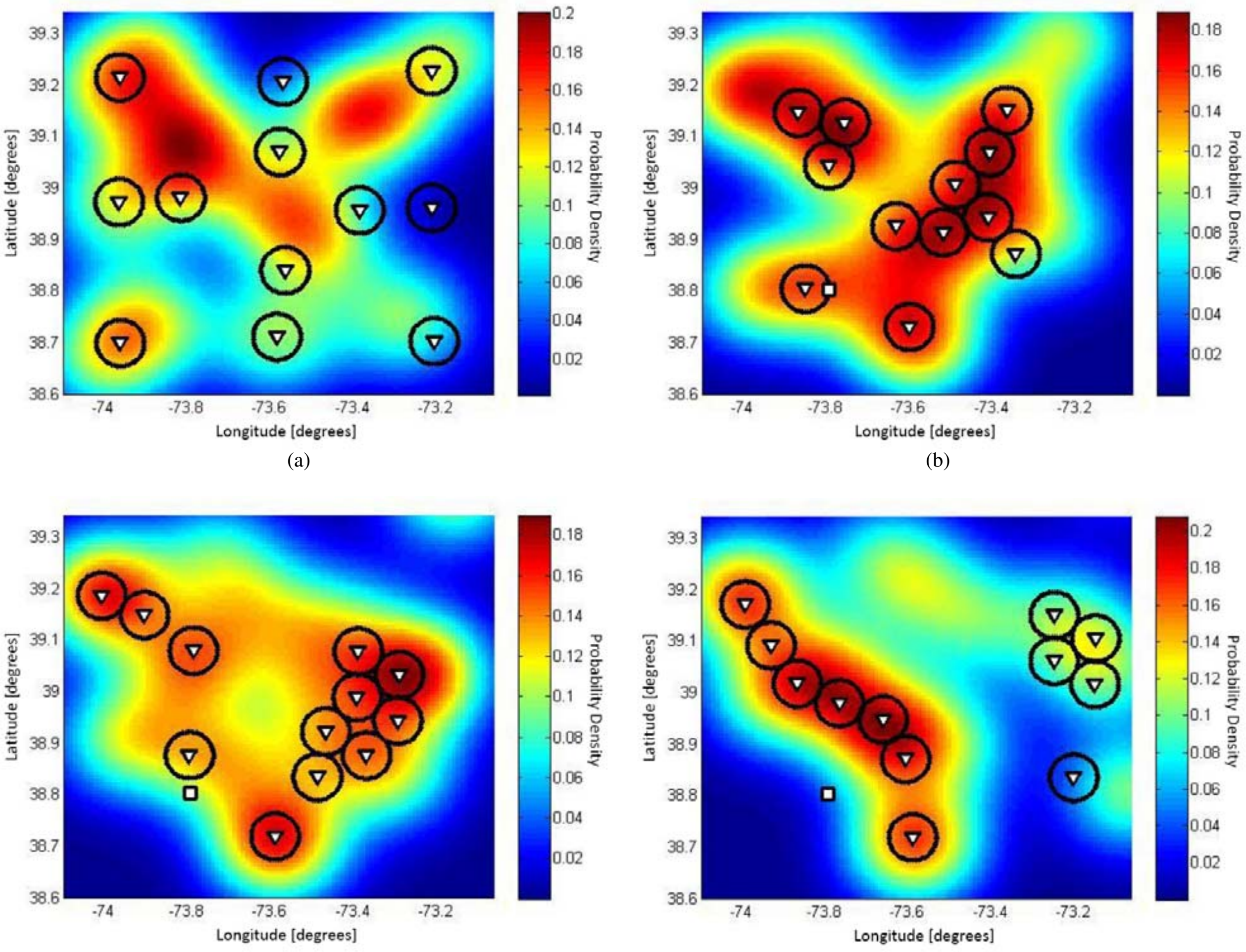

(a)

(b)

(c)

(d)

Fig. 5. The positions of a network of twelve sensors deployed by the potential field approach are plotted at times (a) $t = 0.2$ hours, (b) $t = 3.5$ hours, (c) $t = 6.5$ hours, and (d) $t = 9$ hours, superimposed over the time-varying PDF.

VI. CONCLUSIONS AND FUTURE WORK

This paper presents a methodology to plan the paths of a distributed sensor network in a complex dynamic environment, based on a goal PDF that is parameterized by a time-varying Gaussian mixture. The methodology is based on the potential field approach, and generates a novel potential function by multiplying the goal PDF by a likelihood update model that produces networks with disjoint FOVs. The goal PDF may, therefore, be optimized to meet network or field-level objectives, such as cooperative track detection, that would otherwise be computationally too expensive to optimize with respect to the individual sensors' trajectories. The methodology is applied to an ocean sensor network deployed in an obstacle-populated ROI near the New Jersey coast, and subject to a time-varying current velocity field modeled from real data. The results show that by using the PDF-based potential function, and a function based on potential flow, the sensors follow the PDF while, at the same time, minimizing power required, and avoiding collisions with obstacles that are sensed online.

VII. ACKNOWLEDGMENTS

We gratefully acknowledge Dr. Thomas A. Wettergren at the Naval Undersea Warfare Center for his helpful guidance and suggestions. This research was funded by the Office of Naval Research, Code 321.

REFERENCES

[1] J.-P. LeCadre and G. Souris, "Searching tracks," *IEEE Transactions on Aerospace and Electronic Systems*, vol. 36, no. 4, pp. 1149–1166, 2000.

[2] K. C. Baumgartner and S. Ferrari, "A geometric transversal approach to analyzing track coverage in sensor networks," *IEEE Transactions on Computers*, vol. 57, no. 8, pp. 1113–1128, 2008.

[3] T. A. Wettergren, R. L. Streit, and J. R. Short, "Tracking with distributed sets of proximity sensors using geometric invariants," *IEEE Transactions on Aerospace and Electronic Systems*, vol. 40, no. 4, pp. 1366–1374, October 2004.

[4] T. A. Wettergren, "Performance of search via track-before-detect for distributed sensor networks," *IEEE Transactions on Aerospace and Electronic Systems*, vol. 44, no. 1, pp. 314–325, January 2008.

[5] G. V. Keuk, "Sequential track extraction," *IEEE Transactions on Aerospace and Electronic Systems*, vol. 34, no. 4, pp. 1135–1148, 1998.

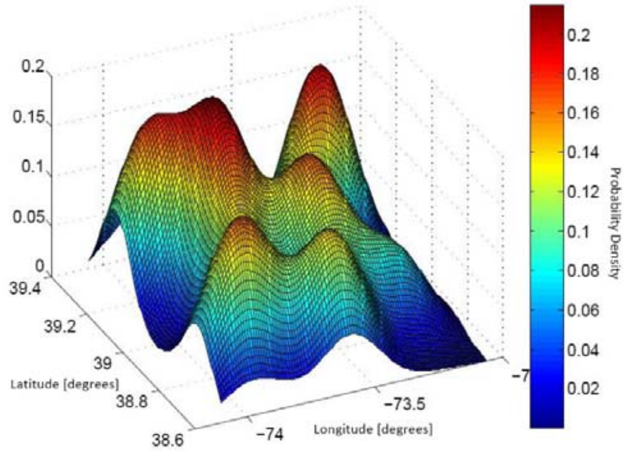

Fig. 4. Gaussian-mixture PDF at $t = 2$ hr.

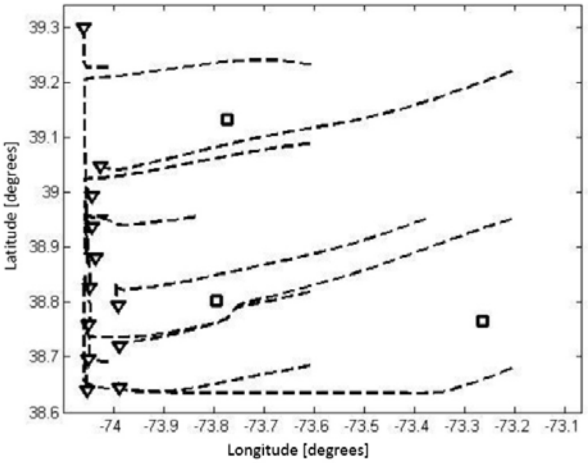

Fig. 6. Sensors trajectories obtained from (21) with $w_f = 0$.

[6] T. A. Wettergren and R. Costa, "Optimal placement of distributed sensors against moving targets," *ACM Transactions on Sensor Networks*, vol. 5, no. 3, p. Article 26, May 2009.

[7] N. Rao, S. Hareti, W. Shi, and S. Iyengar, "Robot navigation in unknown terrains: Introductory survey of non-heuristic algorithms," in *Technical Report ORNL/TM-12410*, Oak Ridge National Laboratory, Oak Ridge, TN, 1993.

[8] Z. Sun and J. Reif, "On robotic optimal path planning in polygonal regions with pseudo-eucledian metrics," *IEEE Transactions on Systems, Man, and Cybernetics - Part A*, vol. 37, no. 4, pp. 925–936, 2007.

[9] S. Ge and Y. Cui, "New potential functions for mobile robot path planning," *IEEE Transactions on Robotics and Automation*, vol. 16, no. 5, 2000.

[10] J. C. Latombe, *Robot Motion Planning*. Kluwer Academic Publishers, 1991.

[11] T. I. Fossen, *Guidance and Control of Underwater Vehicles*. New York, NY: Wiley, 1994.

[12] A. Alvarez, A. Caiti, and R. Onken, "Evolutionary path planning for

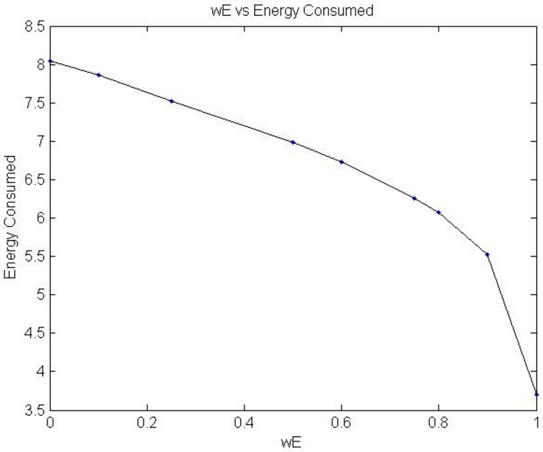

Fig. 7. Energy consumption for various combinations of potential function weights $w_\mathcal{E}$ and $w_\mathcal{E} = 1$.

autonomous underwater vehicles in a variable ocean," *IEEE Journal of Oceanic Engineering*, vol. 29, no. 2, pp. 418–429, 2004.

[13] T. Inanc, S. C. Shadden, and J. E. Marsden, "Optimal trajectory generation in ocean flows," in *Proceedings of the 2005 American Control Conference*, Portland, OR.

[14] R. F. Stengel, *Optimal Control and Estimation*. Dover Publications, Inc., 1986.

[15] M. Chu, H. Haussecker, and F. Zhao, "Scalable information-driven sensor querying and routing for ad hoc heterogeneous sensor networks," *International Journal of High Performance Computing Applications*, vol. 16, no. 3, pp. 293–313, 2002.

[16] R. Urick, *Principles of Underwater Sound*, 3rd ed. McGraw-Hill Book Company, 1983.

[17] K. C. Baumgartner, S. Ferrari, and A. Rao, "Optimal control of an underwater sensor network for cooperative target tracking," *IEEE Journal of Oceanic Engineering*, vol. in press, 2009.

[18] M. S. Bazaraa, H. D. Sherali, and C. M. Shetty, *Nonlinear Programming: Theory and Algorithms*. Hoboken, NJ: Wiley Interscience, 2006.

[19] J. Barraquand, B. Langlois, and J.-C. Latombe, "Numerical potential field techniques for robot path planning," *IEEE Transactions on Systems, Man, and Cybernetics*, vol. 22, no. 2, 1992.

[20] G. Zhang and S. Ferrari, "An adaptive artificial potential function approach for geometric sensing," in *Proc. of the IEEE Conference on Decision and Control*, Shanghai, China, 2010, p. in press.

[21] K. C. Baumgartner, S. Ferrari, and T. Wettergren, "Robust deployment of dynamic sensor networks for cooperative track detection," *IEEE Sensors*, vol. 9, no. 9, pp. 1029–1048, 2009.

[22] P. F. J. Lermusiaux, "Evolving the subspace of the three-dimensional multiscale ocean variability: Massachusetts bay," *Journal of Marine Systems*, vol. 29, 2001.

[23] Mathworks, *MATLAB Neural Network Toolbox*. [Online]. Avaliable: http://www.mathworks.com, 2006, function: trainbr.

[24] H. Lamb, *Hydrodynamics*. Cambridge University Press, 1994.

[25] (2002) COOL, Rutgers University. [Online]. Available: http://marine.rutgers.edu/